

# Gravitational waves from supernova matter

S. Scheidegger, S.C. Whitehouse, R. Käppeli, and M. Liebendörfer

Institute of Physics, Basel University Klingelbergstrasse 82 CH-4056 Basel, Switzerland

E-mail: simon.scheidegger@unibas.ch

**Abstract.** We have performed a set of 11 three-dimensional magnetohydrodynamical core-collapse supernova simulations in order to investigate the dependencies of the gravitational wave signal on the progenitor's initial conditions. We study the effects of the initial central angular velocity and different variants of neutrino transport. Our models are started up from a  $15M_{\odot}$  progenitor and incorporate an effective general relativistic gravitational potential and a finite temperature nuclear equation of state. Furthermore, the electron flavour neutrino transport is tracked by efficient algorithms for the radiative transfer of massless fermions. We find that non- and slowly rotating models show gravitational wave emission due to prompt- and lepton driven convection that reveals details about the hydrodynamical state of the fluid inside the protoneutron stars. Furthermore we show that protoneutron stars can become dynamically unstable to rotational instabilities at  $T/|W|$  values as low as  $\sim 2\%$  at core bounce. We point out that the inclusion of deleptonization during the postbounce phase is very important for the quantitative GW prediction, as it enhances the absolute values of the gravitational wave trains up to a factor of ten with respect to a lepton-conserving treatment.

PACS numbers: 04.30.Db, 95.30.Qd, 97.60.Bw

## 1. Introduction

Stars in the mass range  $8M_{\odot} \lesssim M \lesssim 40M_{\odot}$  end their lives in a core-collapse supernova (CCSN). However, at present the fundamental explosion mechanism, which causes a star to lose its envelope by a yet uncertain combination of factors including neutrino heating, rotation, hydrodynamical instabilities, core g-mode oscillations and magnetic fields, is still under debate (for a review, see e.g. (11)). As strong indications both from theory and observations exist that CCSNe show aspherical, multidimensional features (10; 20), there is a reasonable hope that a small amount of the released binding energy will also be emitted as gravitational waves (GWs), thus delivering us first-hand information about the dynamics and the state of matter at the centre of the star. GW emission from CCSNe were suggested to arise from i) axisymmetric rotational core collapse and bounce (51; 17; 5; 6) ii) prompt-, neutrino-driven postbounce convection and anisotropic neutrino emission (32; 27; 15; 29; 33; 13; 14), iii) protoneutron star (PNS) g-mode oscillations (35) and iv) nonaxisymmetric rotational instabilities (41; 48; 39; 40; 38; 37; 42; 43) For recent reviews with a more complete list of references, see (16; 34). However, only i) can be considered as being well understood as far as the physics of the collapse is concerned, since only these models incorporate all relevant input physics known at present (6) (there are, though, still large uncertainties with respect to the progenitor star, e.g. rotation profiles, magnetic fields, and inhomogeneities from convection). The prediction of all other suggested emission scenarios (ii-iv) still neglect, to a certain extent, dominant physics features due to the diversity and complexity of the CCSN problem on the one hand side and restrictions of available computer power on the other side. Hence, the computational resources were so far either spent on highly accurate neutrino transport (e.g. (21; 36; 29)) while neglecting other physical degrees of freedom such as magnetic fields, or

focus on a general relativistic treatment and/or 3D fluid effects such as accretion funnels, rotation rate and convection, but approximate or even neglect the important micro physics. Only recently have detailed 3D computer models of CCSN become feasible with the emerging power of tens of thousands CPUs unified in a single supercomputer. Such detailed simulations are absolutely indispensable for the following reasons: a) GW astronomy requires not only very sensitive detectors, but also depends on extensive data processing of the detector output on the basis of reliable GW estimates (1). b) The temperatures and densities inside a supernova core exceed the range that is easily accessible by terrestrial experiments. Thus, it will be impossible for the foreseeable future to construct a unique finite temperature equation of state (EoS) for hot and dense matter based on experimentally verified data. Therefore, models with different parameter settings must be run and their computed wave form output then can be compared with actual detector data. Hence, modelling will bridge the gap between theory and measurement and allowing the use of CCSNe as laboratory for exotic nuclear and particle physics (25). In this paper, we will present the GW analysis of a set of 11 three-dimensional ideal magnetohydrodynamical (MHD) core-collapse simulations. We will focus our study on the imprint of 3D nonaxisymmetric features onto the GW signature. Our calculations include presupernova models from stellar evolution calculations, a finite-temperature nuclear EoS and a computationally efficient treatment of deleptonization during the collapse phase. General relativistic corrections to the spherically symmetric Newtonian gravitational potential are taken into account. Moreover, while several models incorporate long-term neutrino physics by means of a leakage scheme, we also present the first results of a model which includes a neutrino transport approximation in the postbounce phase that takes into account both neutrino heating and cooling. As for the progenitor, we systematically investigate the effects of the spatial grid resolution, the neutrino transport physics and the precollapse rotation rate with respect to its influence on the nonaxisymmetric matter dynamics.

This paper is organised as follows. In section 2 we briefly describe the initial model configurations and the numerical techniques employed for their temporal evolution. Furthermore, we review the tools used for the GW and data analysis. Section 3 collects the results of our simulations. Finally, section 4 contains our conclusions and an outlook of our future research.

### *1.1. Description of the magnetohydrodynamical models*

For the 3D Newtonian ideal MHD CCSN simulations presented in this paper, we use the FISH code (12). The gravitational potential is calculated via a spherically symmetric mass integration that includes radial general relativistic corrections (28). The 3D computational domain consists of a central cube of either  $600^3$  or  $1000^3$  cells, treated in equidistant Cartesian coordinates with a grid spacing of 1km or 0.6km. It is, as explained in (42), embedded in a larger spherically symmetric computational domain that is treated by the time-implicit hydrodynamics code ‘Agile’ (23). Closure for the MHD equations is obtained by the softest version of the finite-temperature nuclear EoS of (19). The inclusion of neutrino physics is an essential ingredient of CCSNe simulations, as  $\sim 99\%$  of the released binding energy is converted into neutrinos of all flavours. Their complex interactions with matter (e.g. (11)) are believed to drive the supernova explosion dynamics in the outer layers as well as deleptonizing the PNS to its compact final stage as a neutron star. As the Boltzmann neutrino transport equation can only be numerically solved in a complete form in spherical symmetry on today’s supercomputers (30), our 3D simulations must rely on several feasible approximations which capture the dominant features of the neutrino physics. As for the treatment of the deleptonization during the collapse phase, we apply a simple and computationally efficient  $Y_e$  vs.  $\rho$  parametrization scheme which is based on data from detailed 1D radiation-hydrodynamics calculations (24). For this we use the results obtained with the Agile-Boltztran code (22), including the above-mentioned EoS and the electron capture rates from (2). Around core bounce, this scheme breaks down as it cannot model the neutronization

**Table 1.** Summary of the models' initial conditions and GW related quantities.  $\Omega_{c,i}$  [rads<sup>-1</sup>] is the precollapse central angular velocity, while  $\beta = T/|W|$  is the ratio of rotational to gravitational energy.  $\rho_{c,b}$  [ $10^{14} \text{gcm}^{-3}$ ] is the maximum central density at the time of core bounce.  $E_{GW}$  [ $10^{-9} M_{\odot} c^2$ ] is the energy emitted as GWs.  $f_b$  [Hz] denotes the peak frequency of the GW burst at bounce, while  $f_{TW}$  [Hz] stands for the spectral peak from the narrow band emission caused by a low  $T/|W|$  instability.  $t_f$  [ms] is the time after core bounce when the simulation was stopped.

| <i>Model</i>       | $\Omega_{c,i}$ | $\beta_i$           | $\beta_b$            | $\rho_{c,b}$ | $f_{TW}$ | $E_{GW}$ | $t_f$ |
|--------------------|----------------|---------------------|----------------------|--------------|----------|----------|-------|
| R0                 | 0              | 0                   | 0                    | 4.39         | -        | 0.02     | 130   |
| R0 <sub>IDSA</sub> | 0              | 0                   | 0                    | 4.34         | -        | 0.01     | 81    |
| R1 <sub>HR</sub>   | 0.3            | $0.6 \cdot 10^{-5}$ | $1.7 \cdot 10^{-4}$  | 4.36         | -        | 0.24     | 25    |
| R1 <sub>L</sub>    | 0.3            | $0.6 \cdot 10^{-5}$ | $1.8 \cdot 10^{-4}$  | 4.38         | -        | 0.10     | 93    |
| R2                 | 3.14           | $0.6 \cdot 10^{-3}$ | $1.6 \cdot 10^{-2}$  | 4.27         | -        | 5.5      | 127   |
| R3                 | 3.93           | $1.0 \cdot 10^{-3}$ | $2.3 \cdot 10^{-2}$  | 4.16         | 670      | 14       | 106   |
| R4                 | 4.71           | $1.4 \cdot 10^{-3}$ | $3.2 \cdot 10^{-2}$  | 4.04         | 615      | 35       | 64    |
| R5                 | 6.28           | $2.6 \cdot 10^{-3}$ | $5.2 \cdot 10^{-2}$  | 3.80         | 725      | 59       | 63    |
| R5 <sub>L</sub>    | 6.28           | $2.6 \cdot 10^{-3}$ | $5.1 \cdot 10^{-2}$  | 3.65         | 909      | 214      | 197   |
| R6                 | 9.42           | $5.7 \cdot 10^{-3}$ | $8.6 \cdot 10^{-2}$  | 3.22         | 662      | 77       | 99    |
| R7                 | 12.57          | $1.0 \cdot 10^{-2}$ | $10.2 \cdot 10^{-2}$ | 2.47         | 727      | 12       | 93    |

burst. After core bounce, the neutrino transport thus is tracked for several models via a partial (i.e. a leakage scheme) or full implementation of the isotropic diffusion source approximation scheme (IDSA, (26)). The IDSA decomposes the distribution function  $f$  of neutrinos into two components, a trapped component  $f^t$  and a streaming component  $f^s$ , representing neutrinos of a given species and energy which find the local zone opaque or transparent, respectively. The total distribution function is the sum of the two components,  $f = f^t + f^s$ . The two components are evolved using separate numerical techniques, coupled by a diffusion source term  $\Sigma$ . The source term  $\Sigma$  converts trapped into streaming particles and vice versa. We determine it from the requirement that the temporal change of  $f^t$  has to reproduce the diffusion limit in the limit of small mean free path. Note that our leakage scheme significantly overestimates the deleptonization in and around the neutrinosphere region, as it neglects any absorption of transported neutrinos by discarding the streaming component ( $f^s = 0$ ). The presupernova stellar models stem from Newtonian 1D stellar evolution calculations and hence may not cover all possible states prior to the collapse of a multidimensional star. Therefore we construct the initial conditions of our simulations by a parametric approach. We employ a solar-metallicity  $15M_{\odot}$  progenitor of (50), and set it into rotation according to a shell-type rotation law of (7) with a shellular quadratic cutoff at 500km radius. The initial magnitude of the magnetic field strength for all models is fixed at values suggested by (9).

### 1.2. Gravitational Wave extraction

We employ the Newtonian quadrupole formula in the *first-moment of momentum density formulation* (8) to extract the GWs from our simulation data. Note that the quadrupole formula is not gauge invariant and only valid in the Newtonian slow-motion limit (31). Nevertheless, it was shown by (44) in comparative tests to work sufficiently well compared to more sophisticated methods, as it preserves phase while being off in amplitude by  $\sim 10\%$ .

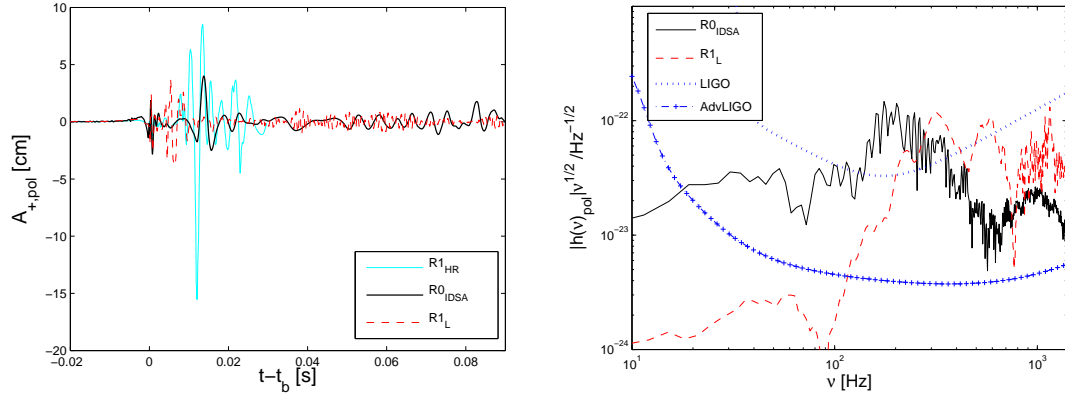


**Figure 1.** **Left:** Time evolution of the GW + polarization for a spectator located at the polar axis (Models  $R1_{HR}$ ,  $R0_{DSA}$  and  $R1_L$ ) **Right:** Corresponding spectral energy distribution of models  $R0_{DSA}$  and  $R1_L$  at a distance of 10kpc compared with the LIGO strain sensitivity and the planned performance of Advanced LIGO (45). Optimal orientation between source and detector is assumed.

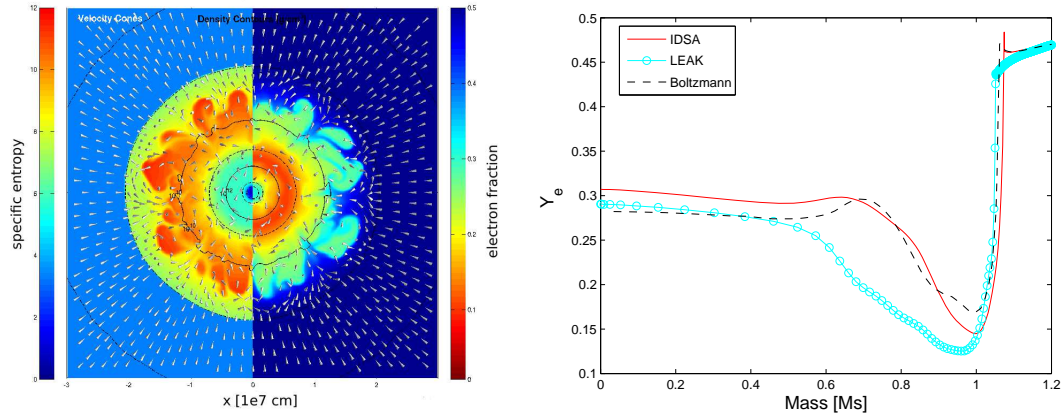


**Figure 2.** **Left:** Model  $R0_{DSA}$ 's specific entropy distribution [ $k_B$ /baryon] (left side) and electron fraction  $Y_e$  (right side) 50ms after core bounce. The innermost  $600^2 \text{ km}^2$  in the x-y plane are displayed. The entropy color bar scales from 0 (blue) to 12 (red). The  $Y_e$  color bar accounts for values from 0 (red) to 0.5 (blue) **Right:** Comparison of the spherically averaged  $Y_e$  profiles of models  $R0_L$  (circled line, 'LEAK'),  $R0_{DSA}$  (solid line, 'IDSA') with the spherically symmetric model G15 (dashed line, 'Boltzmann') as a function of the enclosed mass at 5ms after bounce. Model G15 is based on general relativistic three-flavour neutrino transport (22).

## 2. Results

### 2.1. Non- or slowly rotating core collapse

In order to study the influence of neutrino transport on the stochastic matter dynamics in the early supernova stages ( $t \lesssim 100\text{ms}$  after bounce), without having other different physical parameters interfering, we

carried out three simulations: R0 (purely hydrodynamical postbounce evolution), R1<sub>L</sub> (includes a leakage scheme) and R0<sub>IDSA</sub> (incorporates both neutrino cooling and heating). Non- and slowly rotating progenitors ( $\Omega_{c,i} \leq 0.3 \text{rads}^{-1}$  in our model set) all undergo quasi-spherically symmetric core collapse. As the emission of GWs intrinsically depends on dynamical processes that deviate from spherical symmetry, the collapse phase therefore does not provide any kind of signal, as shown in Fig.1(a) for  $t - t_b < 0$ . However, subsequent pressure-dominated core bounce, where the collapse is halted due to the stiffening of the EoS at nuclear density  $\rho_{nuc} \approx 2 \times 10^{14} \text{gcm}^{-3}$ , launches a shock wave that plows through the infalling layers, leaving behind a negative entropy gradient. Moreover, as soon as the shock breaks through the neutrino sphere  $\sim 5\text{ms}$  after bounce, the immediate burst of electron neutrinos causes a negative lepton gradient at the edge of the PNS. The combination of these two gradients form a convectively unstable region according to the Schwarzschild-Ledoux criterion (18; 49), which in turn induces a GW burst due to this so-called ‘prompt’ convection. A detailed comparison of the models R0, R1<sub>L</sub>, R0<sub>IDSA</sub> shows that all of them follow a similar dynamical behaviour until about 20ms after bounce. At this stage, aspherities leading to GW emission are predominantly driven by the negative entropy gradient and not by the lepton gradient. Hence, the wave trains of all three models, which are based on stochastic processes, fit each other relatively well both in amplitude (several cm) and spectra ( $\sim 150 - 500\text{Hz}$ ). However, ‘prompt’ convection depends, as it was pointed out by (34), not on the negative entropy gradient alone, but also on numerical seed perturbations which are introduced by the choice of the computational grid. Hence, in order to test the dependence of our findings on the spatial resolution, we carried out model R1<sub>HR</sub>. This better resolved simulation shows considerably smaller seed perturbations around  $t - t_b \sim 0$ , as grid alignment effects are better suppressed at core bounce; hence prompt convection then is much weaker and a smaller GW amplitude ( $\sim 50\%$ ) is emitted, as shown in Fig.1(a). However, better numerical resolution also leads to less numerical dissipation in the system, which eases the dynamical effects that follow. Thus, we find for  $\sim 10\text{ms} \lesssim t \lesssim 20\text{ms}$  considerably stronger GW emission in R1<sub>HR</sub> compared to the 1km resolved models, as indicated in Fig.1(a). The three representative simulation results diverge strongly in the later postbounce evolution ( $t \gtrsim 20\text{ms}$ ). Convective overturn causes a smoothing of the entropy gradient. As a result, the GW amplitude in the hydrodynamical model R0 quickly decays ( $t \lesssim 30\text{ms}$  after bounce) and is not revived during the later evolution. On the other hand, the negative radial lepton gradient (see Figs.2(a) and 2(b)) which is caused by the neutronization burst and the subsequent deleptonization, which we model only in R1<sub>L</sub> and R0<sub>IDSA</sub>, now starts to drive convection inside the PNS. For the latter models, the so-called PNS convection (4) exhibits similar maximum amplitudes of  $\sim 1\text{-}2\text{cm}$  (Fig.1(a)), while differing from each other strongly in the corresponding spectra, as displayed in Fig.1(b). R1<sub>L</sub>’s spectrum peaks between  $\sim 600\text{-}1000\text{Hz}$ , while R0<sub>IDSA</sub>’s frequency band peaks at values as low as  $\sim 100\text{Hz}$ . This affects the total energy  $E_{GW}$  emitted ( $\mathcal{O}(10^{-10})M_{\odot}c^2$  vs.  $\mathcal{O}(10^{-11})M_{\odot}c^2$ , see Tab.1), being one order of magnitude higher for R1<sub>L</sub> due to  $dE_{GW}/df \propto f^2$ . We found the key controlling factor of this behaviour to be the radial location of the convectively unstable zones and the related dynamical characteristic timescales  $t_{dyn}$  involved. If we use as rough estimate  $t_{dyn} \sim \Delta_r/\bar{c}_s$ ,  $\ddagger$ , and apply typical values for the models R0<sub>IDSA</sub> and R1<sub>L</sub>, we confirm the obtained values. Furthermore, our leakage scheme significantly overestimates neutrino cooling processes, as one can see in Fig.2(b). There, the convectively unstable layer is extended to radii above nuclear densities, where matter still is opaque for neutrinos and where the local speed of sound assumes values far larger than in the case of model R0<sub>IDSA</sub>. Hence, the dynamical timescale of R1<sub>L</sub> is considerably shorter and the spectral distribution is peaked at higher values. When comparing the results found for model R0<sub>IDSA</sub> with a very recent 2D study of (29), where they carried out one simulation (cf. their model M15LS-2D) with comparable input physics (same  $15M_{\odot}$  progenitor; same underlying finite-temperature EoS) and a very sophisticated neutrino transport scheme, we find very good agreement both in the amplitudes and frequencies. Hence we conclude that the primary ingredient

$\ddagger \bar{c}_s = 1/\Delta_r \int c_s(r)dr$  is the radially averaged sound speed of a convectively unstable layer with a radial extension of  $\Delta_r$ .

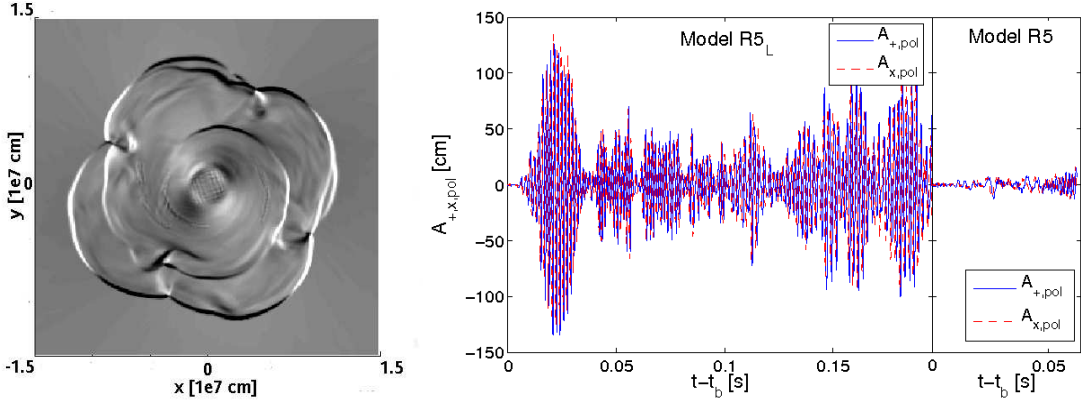


**Figure 3. Left:** Vorticity's z-component  $w_z = (\nabla \times v)_z$  of model  $R5_L$  in the equatorial plane, 29ms after bounce, showing a dominant  $m=1$  mode. The innermost  $300^2 \text{km}^2$  are displayed, and the color is encoded in units of  $[\text{s}^{-1}]$ , ranging from  $-5000$  (white) to  $5000$  (black) **Right:** GW polarizations  $+$  and  $\times$  for models  $R5_L$  and  $R5$  as seen from an observer along the polar axis. Strong nonaxisymmetric dynamics with  $m=2$  components develop right after core bounce. Hence, the two polarizations are shifted by a quarter cycle, as one could expect from GWs emitted by a spinning bar.

for supernova simulations which attempt a quantitative prediction of GWs from ‘prompt’ and early PNS convection ( $t \lesssim 100\text{ms}$  after bounce) is the accurate radial location and size of convectively unstable layers. It defines the dynamical behaviour and timescale of overturning matter in this early supernova stage.

## 2.2. Rotational core collapse & nonaxisymmetric instability at low $T/|W|$

Recently it has been argued based on numerical simulations of equilibrium neutron star models or full core-collapse simulations that differentially rotating PNS can be subject to non-axisymmetric rotational instabilities (see Fig.3(a)) at  $\beta$  values ( $\hat{=} T/|W|$ , the ratio of rotational to gravitational energy) far below the ones known from the classical dynamical bar mode instability with a threshold of  $\beta_{dyn} = 27\%$ , or the secular instability, which is triggered at  $\beta_{sec} \sim 14\%$  (46), leading to strong, narrow-band GW emission, as displayed in Fig.3(b) (3; 37; 42). At present little is known about the true nature of the so-called low  $T/|W|$  instability. Previous work has so far failed to establish (for example) an analytical instability criterion, as was pointed out by (34). We addressed two relevant questions regarding the so-called ‘low  $T/|W|$ ’ instability in the context of stellar core collapse: i) Which is the minimum  $\beta$  value required in self-consistent core-collapse simulation to trigger the onset of the instability? This is important to know, since most stars which undergo a core collapse rotate only slowly (9); furthermore, it was pointed out by (6) that even fast rotating PNS can never accrete enough angular momentum to reach the  $\beta_{dyn}$  value required for the onset of the classical bar mode instability. ii) How does the inclusion of deleptonization in the postbounce phase quantitatively alter the GW signal? So far, 3D models have not included spectral neutrino physics in the postbounce phase. To study i), we systematically change the rotation rate while keeping the other model parameters fixed. The minimum  $T/|W|$  value we found in our parameter range to trigger the instability was  $\beta_b \sim 2.3\%$  at core bounce (model R3), which is considerably lower than seen in previous studies ((37) found  $\beta_b \sim 9\%$ , while (42) found  $\beta_b \sim 5\%$ ). Furthermore, we find that centrifugal forces set a limit to the maximum frequency of the GW signal around  $\sim 900\text{Hz}$ . The faster the initial rotation rate, the stronger the influence of centrifugal forces, which slow down the postbounce advection of angular momentum onto the PNS. The result is a

slower rotation rate, a lower pattern speed and thus GW emission at lower frequencies (see Tab.1). In order to address ii), we carried out ‘leakage’ model R5<sub>L</sub>. This model shows 5-10 × larger maximum amplitudes due to the nonaxisymmetric dynamics compared to its hydrodynamical counterpart R5 that neglects neutrino cooling (see Fig. 3(b)). This suggests that the treatment of postbounce neutrino cooling plays an important role when it comes to the quantitative prediction of GW signals from a low  $\beta$  instability. The neutrino cooling during the postbounce phase leads to a more compact PNS with a shorter dynamical timescale compared to the purely hydrodynamical treatment. This in turn is reflected in the dynamical evolution. The shock wave stalls at considerably smaller radii and becomes more quickly unstable to azimuthal fluid modes. Since there is much more matter in the unstable region of this model, the unstable modes grow faster, causing the emission of much more powerful GWs. However, we again point out that our leakage scheme overestimates the compactification of the PNS due to neutrino cooling. The ‘reality’ for the strength of GW emission therefore should lay in between the results from the pure hydrodynamical- and leakage treatment.

### 3. Summary and outlook

We have presented the GW signature of eleven 3D core-collapse simulations with respect to variations in the spatial grid resolution, the underlying neutrino transport physics and the initial rotation rate. Our results show that in case of non- and slowly rotating models the GWs emitted during the first 20ms after bounce are predominantly due to entropy driven ‘prompt’ convection. It turns out that the crucial parameter to study this stochastic phenomenon is the choice of the spatial resolution and not the inclusion of a neutrino transport scheme. This parameter has a twofold effect: Firstly, it governs the influence of numerical noise, since a better resolution leads to lower numerical seed perturbations and thus smaller grid alignment effects. Therefore, the GW amplitude right at core bounce is smaller for higher spatial resolution. Secondly, it enhances the ability to follow dynamical features, as better numerical resolution causes less numerical dissipation in the system, which eases the dynamical effects which follow, leading to larger GW amplitudes after the core bounce compared to less resolved models. The lepton driven convection is the central engine for the later dynamical postbounce evolution of the PNS ( $t \gtrsim 20\text{ms}$ ) and hence the GW emission. Our findings and comparisons with state of the art 2D simulations of (29) suggest that the radial location and size of the convectively unstable layers are the key controlling factor for the outcome of the GW prediction, as they define the timescale and the dynamical behaviour of the overturning matter. Here we find a large sensitivity to the numerical approach of the neutrino transport scheme. In our rotational core-collapse simulations, nonaxisymmetric dynamics develops for models with a rotation rate of  $\beta_b \gtrsim 2.3\%$  at core bounce. Beyond this value, which is considerably lower than found in previous studies (e.g. (37; 42)), all models become subject to the ‘low  $T/|W|$ ’ instability of dominant  $m=1$  or  $m=2$  character within several ms after bounce (Fig.3(a)). The fact that the effectively measured GW amplitude scales with the number of GW cycles  $N$  as  $h_{eff} \propto h \sqrt{N}$  (47) suggests that the detection of such a signal is tremendously enhanced. Moreover, we point out that the inclusion of deleptonization during the postbounce phase causes a compactification of the PNS which enhances the absolute values of the GW amplitudes up to a factor of ten with respect to a lepton-conserving treatment.

The major limitation of our code now is in the monopole treatment of gravity, since it cannot account for spiral structures, which could be reflected in GW. We are currently working on the improvement of this issue. Furthermore, the IDSA includes at present only the dominant reactions relevant to the neutrino transport problem (see (26) for details). Future upgrades will also include contributions from electron-neutrino scattering, which are indispensable during the collapse phase. The inclusion of this reaction will also make the cumbersome switch of the parametrization to the IDSA at bounce obsolete. Finally, we work on the inclusion of  $\mu$  and  $\tau$  neutrinos, which are very important for the cooling of the PNS to its final stage

as neutron star.

### Acknowledgments

The authors would like to thank C. D. Ott for stimulating and useful discussions and F.-K. Thielemann for his support. This work was supported by a grant from the Swiss National Supercomputing Centre-CSCS under project ID s168. We acknowledge support by the Swiss National Science Foundation under grant No. 200020-122287 and PP00P2-124879. Moreover, this work was supported by CompStar, a Research Networking Programme of the European Science Foundation. Further thanks go to John Biddiscombe and Sadaf Alam from the Swiss Supercomputing Centre CSCS for the smooth and enjoyable collaboration.

### References

- [1] Abbott, B. et al. (LIGO Scientific) 2009 LIGO: the Laser Interferometer Gravitational-Wave Observatory Reports on Progress in Physics, 72, 076901–+, 7
- [2] S. W. Bruenn. Stellar core collapse - Numerical model and infall epoch. *ApJS*, 58:771–841, August 1985.
- [3] P. Cerdá-Durán, V. Quilis, and J. A. Font. AMR simulations of the low T/—W— bar-mode instability of neutron stars. *Computer Physics Communications*, 177:288–297, August 2007.
- [4] L. Dessart, A. Burrows, E. Livne, and C. D. Ott. Multidimensional Radiation/Hydrodynamic Simulations of Proto-Neutron Star Convection. *ApJ*, 645:534–550, July 2006.
- [5] H. Dimmelmeier, C. D. Ott, H.-T. Janka, A. Marek, and E. Müller. Generic Gravitational-Wave Signals from the Collapse of Rotating Stellar Cores. *Physical Review Letters*, 98(25):251101–+, June 2007.
- [6] H. Dimmelmeier, C. D. Ott, A. Marek, and H.-T. Janka. Gravitational wave burst signal from core collapse of rotating stars. *Phys. Rev. D*, 78(6):064056–+, September 2008.
- [7] Eriguchi Y, Mueller E. A general computational method for obtaining equilibria of self-gravitating and rotating gases. *A&A*. 1985 May;146:260–268.
- [8] L. S. Finn and C. R. Evans. Determining gravitational radiation from Newtonian self-gravitating systems. *ApJ*, 351:588–600, March 1990.
- [9] Heger A, Woosley SE, Spruit HC. Presupernova Evolution of Differentially Rotating Massive Stars Including Magnetic Fields. *ApJ*. 2005 Jun;626:350–363.
- [10] Herant M, Benz W, Hix WR, Fryer CL, Colgate SA. Inside the supernova: A powerful convective engine. *ApJ*. 1994 Nov;435:339–361.
- [11] H.-T. Janka, K. Langanke, A. Marek, G. Martínez-Pinedo, and B. Müller. Theory of core-collapse supernovae. *Phys. Rep.*, 442:38–74, April 2007.
- [12] R. Kaeppli, S. C. Whitehouse, S. Scheidegger, U. -. Pen, and M. Liebendoerfer. FISH: A 3D parallel MHD code for astrophysical applications. *ArXiv e-prints*: 0910.2854
- [13] K. Kotake, W. Iwakami, N. Ohnishi, and S. Yamada. Ray-Tracing Analysis of Anisotropic Neutrino Radiation for Estimating Gravitational Waves in Core-Collapse Supernovae. *ApJ*, 704:951–963, October 2009.
- [14] K. Kotake, W. Iwakami, N. Ohnishi, and S. Yamada. Stochastic Nature of Gravitational Waves from Supernova Explosions with Standing Accretion Shock Instability. *ApJ*, 697:L133–L136, June 2009.



- [15] K. Kotake, N. Ohnishi, and S. Yamada. Gravitational Radiation from Standing Accretion Shock Instability in Core-Collapse Supernovae. *ApJ*, 655:406–415, January 2007.
- [16] K. Kotake, K. Sato, and K. Takahashi. Explosion mechanism, neutrino burst and gravitational wave in core-collapse supernovae. *Reports of Progress in Physics*, 69:971–1143, 2006.
- [17] Kotake K, Yamada S, Sato K, Sumiyoshi K, Ono H, Suzuki H. Gravitational radiation from rotational core collapse: Effects of magnetic fields and realistic equations of state. *Phys. Rev. D*. 2004 Jun;69(12):124004–+.
- [18] L. D. Landau and E. M. Lifshitz. *Fluid mechanics*. Course of theoretical physics, Oxford: Pergamon Press, 1959, 1959.
- [19] J. M. Lattimer and F. D. Swesty. A generalized equation of state for hot, dense matter. *Nucl. Phys. A*, 535:331–376, December 1991.
- [20] D. C. Leonard, A. V. Filippenko, M. Ganeshalingam, F. J. D. Serduke, W. Li, B. J. Swift, A. Gal-Yam, R. J. Foley, D. B. Fox, S. Park, J. L. Hoffman, and D. S. Wong. A non-spherical core in the explosion of supernova SN 2004dj. *Nature*, 440:505–507, March 2006.
- [21] Liebendörfer M, Messer OEB, Mezzacappa A, Bruenn SW, Cardall CY, Thielemann F. A Finite Difference Representation of Neutrino Radiation Hydrodynamics in Spherically Symmetric General Relativistic Spacetime. *ApJS*. 2004 Jan;150:263–316.
- [22] Liebendörfer M, Rampp M, Janka H, Mezzacappa A. Supernova Simulations with Boltzmann Neutrino Transport: A Comparison of Methods. *ApJ*. 2005 Feb;620:840–860.
- [23] Liebendörfer M, Rosswog S, Thielemann F. An Adaptive Grid, Implicit Code for Spherically Symmetric, General Relativistic Hydrodynamics in Comoving Coordinates. *ApJS*. 2002 Jul;141:229–246.
- [24] Liebendörfer M. A Simple Parameterization of the Consequences of Deleptonization for Simulations of Stellar Core Collapse. *ApJ*. 2005 Nov;633:1042–1051.
- [25] M. Liebendörfer, T. Fischer, M. Hempel, A. Mezzacappa, G. Pagliara, I. Sagert, J. Schaffner-Bielich, S. Scheidegger, F.-K. Thielemann, and S. C. Whitehouse. Supernovae as Nuclear and Particle Physics Laboratories. *Nuclear Physics A*, 827:573–578, August 2009.
- [26] M. Liebendörfer, S. C. Whitehouse, and T. Fischer. The Isotropic Diffusion Source Approximation for Supernova Neutrino Transport. *ApJ*, 698:1174–1190, June 2009.
- [27] Müller E, Rampp M, Buras R, Janka H, Shoemaker DH. Toward Gravitational Wave Signals from Realistic Core-Collapse Supernova Models. *ApJ*. 2004 Mar;603:221–230.
- [28] Marek A, Dimmelmeier H, Janka H, Müller E, Buras R. Exploring the relativistic regime with Newtonian hydrodynamics: an improved effective gravitational potential for supernova simulations. *A&A*. 2006 Jan;445:273–289.
- [29] A. Marek, H.-T. Janka, and E. Müller. Equation-of-state dependent features in shock-oscillation modulated neutrino and gravitational-wave signals from supernovae. *A&A*, 496:475–494, March 2009.
- [30] A. Mezzacappa. The Core Collapse Supernova Mechanism: Current Models, Gaps, and the Road Ahead. In M. Turatto, S. Benetti, L. Zampieri, and W. Shea, editors, *ASP Conf. Ser. 342: 1604-2004: Supernovae as Cosmological Lighthouses*, pages 175–+, December 2005.
- [31] C. W. Misner, K. S. Thorne, and J. A. Wheeler. *Gravitation*. San Francisco: W.H. Freeman and Co., 1973, 1973.
- [32] Mueller E, Janka HT. Gravitational radiation from convective instabilities in Type II supernova explosions. *A&A*. 1997 Jan;317:140–163.

- [33] Murphy JW, Ott CD, Burrows A. A Model for Gravitational Wave Emission from Neutrino-Driven Core-Collapse Supernovae. *ApJ*. 2009 Dec;707:1173–1190.
- [34] C. D. Ott. TOPICAL REVIEW: The gravitational-wave signature of core-collapse supernovae. *Classical and Quantum Gravity*, 26(6):063001–+, March 2009.
- [35] C. D. Ott, A. Burrows, L. Dessart, and E. Livne. A New Mechanism for Gravitational-Wave Emission in Core-Collapse Supernovae. *Physical Review Letters*, 96(20):201102–+, May 2006.
- [36] C. D. Ott, A. Burrows, L. Dessart, and E. Livne. Two-Dimensional Multiangle, Multigroup Neutrino Radiation-Hydrodynamic Simulations of Postbounce Supernova Cores. *ApJ*, 685:1069–1088, October 2008.
- [37] C. D. Ott, H. Dimmelmeier, A. Marek, H.-T. Janka, I. Hawke, B. Zink, and E. Schnetter. 3D Collapse of Rotating Stellar Iron Cores in General Relativity Including Deleptonization and a Nuclear Equation of State. *Physical Review Letters*, 98(26):261101–+, June 2007.
- [38] C. D. Ott, H. Dimmelmeier, A. Marek, H.-T. Janka, B. Zink, I. Hawke, and E. Schnetter. Rotating collapse of stellar iron cores in general relativity. *Classical and Quantum Gravity*, 24:139–+, June 2007.
- [39] C. D. Ott, S. Ou, J. E. Tohline, and A. Burrows. One-armed Spiral Instability in a Low- $T/W$ —Postbounce Supernova Core. *ApJ*, 625:L119–L122, June 2005.
- [40] S. Ou and J. E. Tohline. Unexpected Dynamical Instabilities in Differentially Rotating Neutron Stars. *ApJ*, 651:1068–1078, November 2006.
- [41] M. Saijo, T. W. Baumgarte, and S. L. Shapiro. One-armed Spiral Instability in Differentially Rotating Stars. *ApJ*, 595:352–364, September 2003.
- [42] S. Scheidegger, T. Fischer, S. C. Whitehouse, and M. Liebendörfer. Gravitational waves from 3D MHD core collapse simulations. *A&A*, 490:231–241, October 2008.
- [43] S. Scheidegger, R. Kaeppli, S. C. Whitehouse, T. Fischer, and M. Liebendoerfer. The influence of model parameters on the prediction of gravitational wave signals from stellar core collapse. *ArXiv e-prints*: 1001.1570
- [44] M. Shibata and Y.-I. Sekiguchi. Gravitational waves from axisymmetrically oscillating neutron stars in general relativistic simulations. *Phys. Rev. D*, 68(10):104020–+, November 2003.
- [45] Shoemaker, D. 2007, private communication
- [46] Tassoul JL. Theory of rotating stars. Tassoul JL, editor; 1978.
- [47] Hawking SW, Israel W. Three Hundred Years of Gravitation. Three Hundred Years of Gravitation; 1989.
- [48] A. L. Watts, N. Andersson, and D. I. Jones. The Nature of Low  $T/W$ — Dynamical Instabilities in Differentially Rotating Stars. *ApJ*, 618:L37–L40, January 2005.
- [49] J. R. Wilson and R. W. Mayle. Convection in core collapse supernovae. *Phys. Rep.*, 163:63–77, 1988.
- [50] S. E. Woosley and T. A. Weaver. The evolution and explosion of massive stars. ii. explosion hydrodynamics and nucleosynthesis. 101:181, 1995.
- [51] Zwerger T, Mueller E. Dynamics and gravitational wave signature of axisymmetric rotational core collapse. *A&A*. 1997 Apr;320:209–227.